A temperature-sensitive RFID tag for the identification of cold chain failures

F. Vivaldi[a *], B. Melai[a], A. Bonini[a], N. Poma[a], P. Salvo[b], A. Kirchhain[a], S. Tintori[a], A. Bigongiari[c], F. Bertuccelli[c], G. Isola[c], F. Di Francesco[a]

[a] Department of Chemistry and Industrial Chemistry, University of Pisa, via Giuseppe Moruzzi 13, 56124, Pisa, Italy.

[b] Institute of Clinical Physiology (IFC) of National Research Council (CNR), Via Moruzzi 1, 56124, Pisa, Italy.

[c] Caen RFID srl, Via Vetraia 11, 55049, Viareggio, Italy.

* Corresponding author, *federicomaria.vivaldi@phd.unipi.it*

Abstract

Quality and safety of the cold chain undergo strict international regulations that identify storage and shipping temperatures. In fact, the improper handling and transportation of temperature-sensitive products such as food and pharmaceuticals may have harmful effects on human health and a negative economic impact. A passive RFID tag modified with a copper-doped ionic liquid was used to detect the crossing of a temperature threshold (8 °C) during the shipping of medical products. The tag was insensitive to humidity variations and irreversibly changed its status once temperature exceeded the ionic liquid melting point, which can be tuned by changing the concentration of dopant.

Keywords: cold chain; RFID; ionic liquid; temperature sensor; shipment control; perishable goods

1. Introduction

The global market of perishable and temperature-sensitive goods such as pharmaceuticals, medical products and fresh food is constantly growing at a compound annual growth rate (CAGR) of about 7.7% [1]. Other analysists foresee a CAGR of 17.9% from 2019 to 2026 [2]. The transportation management needs sophisticated software and procedures to handle the delivery and provide a high quality service to the customers. For a successful logistic platform, the implementation of an effective cold chain system is crucial to keep temperature-sensitive products in optimal storage and transport conditions. A cold chain can contain a high density of nodes designed to keep goods within a safe temperature range uninterruptedly before the products reach consumers [3]. National and international regulations and directives provide shipping temperature intervals for storage and transportation that depend on the characteristics of the goods [4,5]. For example, most temperature-sensitive medical products must be kept at 2–8 °C [6], fresh fish at 0-4 °C or at -18–-15 °C if frozen [7], meat at -25 °C or colder, and fruits like bananas between 12 and 16 °C [8]. However, several factors such as packaging failure, human error, equipment malfunction and non-uniform cooling standards across countries can make cold chain fail. These risks are an important health threat and sources of economic losses. For example, the improper handling and transportation account for an estimated annual loss of more than $750 billion in the food market [9], whereas Biopharma companies annually spend $260 billion to ensure the efficacy of their cold chain logistics [10]. Therefore, there is a growing demand of low cost and easy-to-use temperature sensors capable of tracking the cold chain to improve management and identify failures.

Different solutions for temperature monitoring and identification of cold chain failures have been described in the scientific literature or are commercially available. Time-temperature indicators (TTIs) are lightweight and inexpensive (few euro cents per piece) colorimetric tags that undergo a mechanical, microbiological, chemical or enzymatic change when temperature exceeds a predefined threshold [11]. There are several off-the-shelf TTIs, e.g. CheckPoint™, 3M™ MonitorMark™, Fresh-Check®, TT Sensor™ and Keep-it®, which can be used for different temperature ranges [12]. Since the color change is irreversible, TTIs are disposable; an electronic indicator to improve the color reading [13] is sometimes provided. Although available since 1970s, TTIs have never gained a wide market penetration because of their low accuracy due to the ambiguous quantification of color change [14].

Thermistors, resistance temperature detectors (RTDs) and thermocouples are widely used for monitoring temperature in many fields, such as industrial and manufacturing processes, food and beverage products, environment control, consumer electronics, and healthcare [15–18]. These temperature sensors can be coupled or integrated in a datalogger for a continuous monitoring. Thermocouples can be inaccurate if exposed to moisture, voltage noise, or large variations in ambient temperature, whereas RTDs are expensive and rarely used in cold chain logistics [19,20]. Due to good accuracy and small size [21–24], many temperature-tracking systems prefer thermistors, but those allowing high accuracy measurements are expensive, fragile and need filters or DC voltage because of their high resistance [25]. In recent years, other techniques have been investigated to measure temperature in cold chain products, e.g. infrared thermography and fluorescence, but their use is still limited because of high cost, limited applicability and inaccuracy [26–28].

Although the aforementioned sensors and technologies allowed temperature measurement, the cold chain management system had poor access to data during shipment before the adoption of wireless data transfer. Technologies such as Bluetooth and Radio frequency identification (RFID) allow the temperature monitoring without a direct access of packagings. RFID is widely adopted in logistics because it is an affordable technology that allows to track the refrigeration status in real-time from the production until the sale of the product [29,30]. Active and semi-passive RFID tags use a power source, typically a battery, whereas passive tags are powered by the external electromagnetic field emitted from the reader. Passive RFID tags are usually preferred for product traceability as they are low cost and long lasting. They consists of a microchip and an antenna [31] and are accessed by a reader operating in the low frequency (125 and 134 KHz), high frequency (13.56 MHz), ultra-high frequency (UHF) (860 – 960 MHz) and microwave (2.4 GHz and 5.8 GHz) bands. Higher frequencies allow the reader to connect with tags in a broader range, from a few centimeters up to several meters [32].

Several papers in literature have described RFID tags using commercial or integrated silicon sensors to monitor temperature in cold chain systems [29,33–39]. Bhattacharyya et al. [40] fabricated a temperature-sensitive polymer that actuates a metal plate between two RIFD tags. In this paper, we describe the fabrication of a passive RFID tag modified with an ionic liquid, [C_{12}mim][Tf_2N], to sense temperature. Ionic liquids are salts in liquid state at temperatures lower than 100 °C [41] that can be used to fabricate different types of sensors [42], whose melting temperature can be modified by the selection of the cation/anion pair [43]. Our sensor exploits the melting of copper-doped [C_{12}mim][Tf_2N] (Cu-IL) to change the status of a tag and identify failures in the cold chain.

2. Materials and Methods

2.1. Reagents and Materials

1-methylimidazole (purity 98%), lithium bis(trifluoromethanesulfonyl)imide (purity 99%) and bis(trifluoromethanesulfonyl)imide (99% purity) were purchased from Iolitec. 1-Bromododecane (purity 97 %) and dichloromethane (purity 99%), sodium chloride, magnesium nitrate and potassium acetate were purchased from Sigma Aldrich. Copper Oxide (II) was purchased from Carlo Erba.

2.2. Synthesis of the [C_{12}mim][Tf_2N]

The synthesis of [C_{12}mim][Tf_2N] was performed in a two-step reaction. Figure 1 shows the formation of the bromine ionic liquid by the addition of a halogen alkane to a methyl imidazole center. Two aliquots of 1-methylimidazole (10 mL, 0.1218 mol) and deionized water (20 mL) were added to 28 mL of 1-bromododecane (0.1218 mol). The mixture was heated and refluxed for 12 h until a unique phase was obtained.

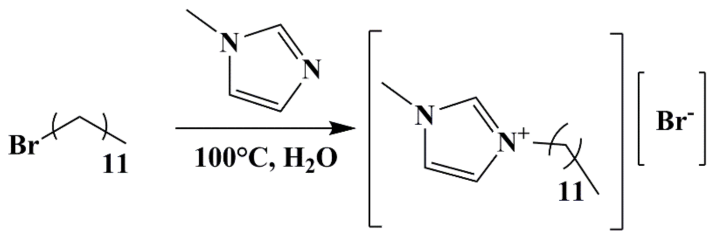

Fig. 1. Synthesis of [C_{12}mim][Br].

In the second step, the anion was exchanged with lithium bis(trifluoromethanesulfonyl)imide (Fig. 2). An aliquot of 5.152 g Li(Tf_2N) (0.0179 mol) was added to 20 mL of deionized water whereas [C_{12}mim][Br^-] was supplemented under magnetic stirring at room temperature. After the addition of 30 mL of dichloromethane, the solution was stirred for 2 h at 40 °C. The organic phase was extracted removing LiBr after five washing cycles with deionized water. Then, the organic phase was dried under vacuum for 2 h at 60 °C in order to remove the organic solvent and the remaining water.

NMR analysis was performed on the synthesized ionic liquid with a Bruker Advance DRX 400:

1H NMR (401 MHz, C_6D_6), δ (ppm): 8.70 (s, 1H), 7.54 (s, 1H), 7.47 (s, 1H), 4.24 (t, J = 7.1 Hz, 2H), 3.96 (s, 3H), 1.95 (s, 2H), 1.39 (d, J = 20.5 Hz, 16H), 0.96 (t, J = 6.5 Hz, 3H).

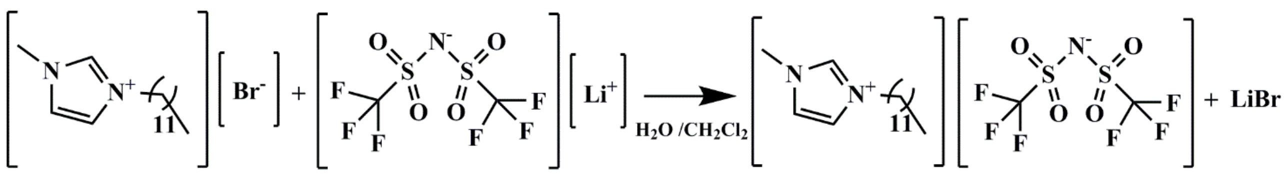

Fig. 2. Anion exchange with lithium bis(trifluoromethanesulfonyl)imide to obtain the hydrophobic ionic liquid [C_{12}mim][Tf_2N].

2.3. Preparation of Cu(Tf_2N)$_2$ and doped ionic liquid

A solution of $Cu(Tf_2N)_2$ was prepared by mixing 2.303 g of copper oxide (0.0289 mol) with 20.003 g of bis(trifluorometilsulfonil)immide (0.05692 mol) in 20 mL of deionized water. After stirring at room temperature overnight, the solution was filtered to remove any excess of copper oxide. The $Cu(Tf_2N)_2$ solution and the$[C_{12}mim][Tf_2N]$ were mixed (molar ratio 0.5) to obtain Cu-IL. Cu-IL was kept under vacuum at room temperature for about 6 h to remove excess water.

2.4. Characterization

In order to calculate the melting and freezing point of the ionic liquids, Differential Scan Calorimetry (DSC) was performed under nitrogen flux (80 mL/min) with a DSC228e Mettler Toledo equipped with a cooling system. The melting and freezing points of Cu-IL were extrapolated from the regression line fitting the onset temperatures at different scan rates (5, 10 and 20 °C/min) calculated by the STARe software (Mettler Toledo). Two identical aluminum pans were used as sample holder and reference for the analysis, respectively.

The amount of water contained in each sample was assessed by a thermogravimetric analysis (TGA, Q5000, TA instruments, heating rate 20 °C/min). Flasks at controlled humidity were prepared as previously reported [44]. Briefly, saturated solutions of potassium acetate, magnesium nitrate and sodium chloride were prepared to obtain relative humidity levels of 22.5, 52.9 and 75.3% at room temperature (25 °C).

2.5. Working principle of the RFID tag

The UHF RFID tag mounts an UCODE G2iM+ transponder (NXP) that can detect the open/closed circuit state between two pads (Figure 3). A drop (10 µL) of Cu-IL is cast between the pads onto the RFID pads kept at low temperature (-40 °C). The instant freezing of the drop avoids any electrical connection between the tracks. Once the transponder is activated from the reader (R1260I SLATE

RFID UHF desktop reader, CAEN RFID), the chip injects a current pulse (amplitude 300 nA, duration 200 μs) through the pads. The integrated circuit detects a closed or an open circuit if the resistance across the pads is lower than 2 MΩ or higher than 20 MΩ, respectively. The status of the contact is stored inside transponder's memory and can be retrieved by the reader. If temperature rises above the Cu-IL melting point, the drop melts and short-circuits the pads, so that the transponder detects a switch from the open to the closed state.

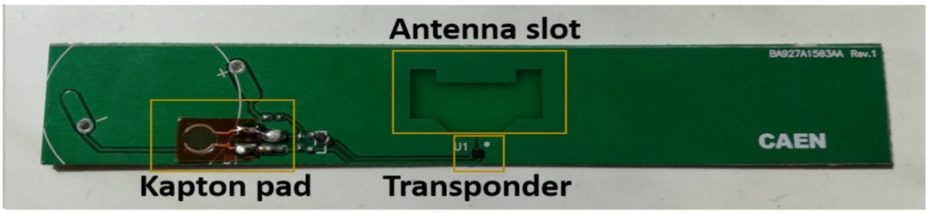

Figure 3. An illustrative Cu-IL RFID tag.

2.6. Electrochemical impedance spectroscopy analysis

The Cu-IL impedance over time was recorded using a potentiostat (Palmsens 4, Palmsens) in a two-electrode configuration and a dedicated software (PSTrace, Palmsens). Table 1 shows the parameters used for electrochemical impedance spectroscopy (EIS). Temperature was monitored by a thermistor (NTC2.2K3359I, Betatherm).

Table 1. Settings for the electrochemical impedance spectroscopy.

Scan type	**Fixed potential**
E_{dc}	0.0 V
E_{ac}	0.01 V
t_{run}	1000 s
Frequency type	Fixed frequency
Frequency	10000 Hz

3. Results and Discussion

3.1. DSC and TGA thermograms

Figure 4 shows the DSC thermogram of the Cu-IL. The peaks at about 10 °C are related to the melting of Cu-IL, whereas freezing points are close to -40 °C due to the typical undercooling of these compounds [45]. Several additional smaller peaks can be noticed that are likely related to glass transitions due to ion reorganization within the solid structure [46].

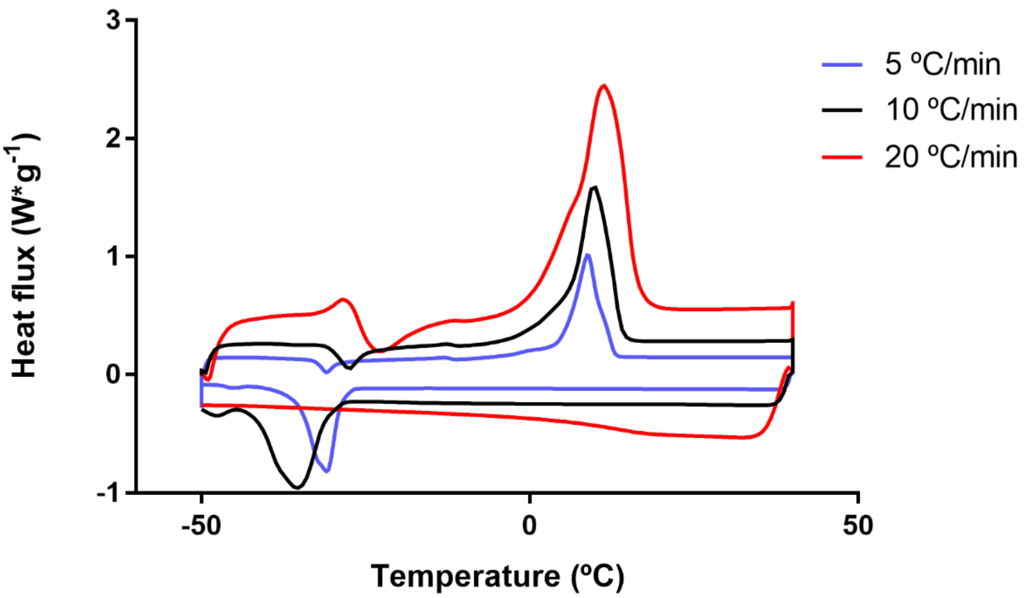

Figure 4. DSC thermograms of Cu-IL at three different temperature scan rates.

Figure 4 also shows a dependence of phase transition temperatures from the temperature scan rate, so that the most accurate temperature values are those obtained with extremely slow variations of temperature. Figure 5 shows the extrapolation of the Cu-IL melting and freezing points, i.e. 8.6 and -35.3 °C, respectively, by regression from the onset temperature values estimated at different temperature scan rates. Since the optimal temperature for refrigerated products ranges between 2-8 °C [47], the melting point of Cu-IL was set at the upper boundary to verify if the cold chain was preserved.

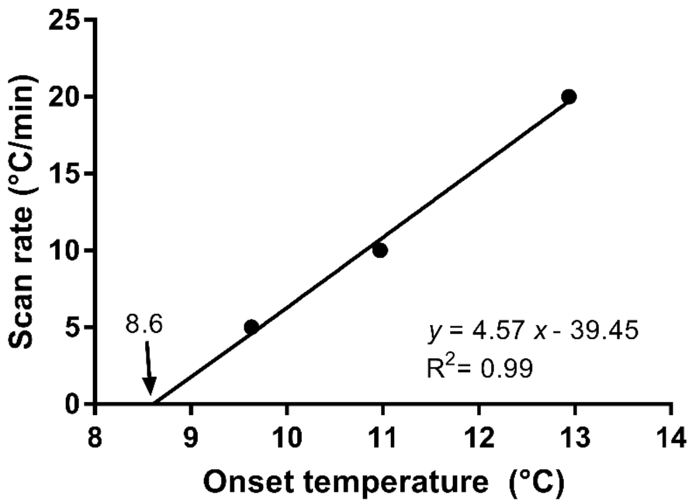

Figure 5. Extrapolation of the Cu-IL melting points by regression from the onset temperature values estimated at different temperature scan rates.

The supercooling effect of Cu-IL (ΔT > 43.9 °C) prevents re-freezing, and its combination with the spreading of the drop makes the process irreversible.

Since ionic liquids tend to absorb water [48] and this can modify the freezing and melting points, the behavior of the Cu-IL was tested at three different levels of relative humidity (RH). Figure 6 shows three similar Cu-IL thermograms at 22.5%, 52.9% and 75.3% RH. The weight loss in the range [25, 100] °C (Table 2) was attributed to the loss of water from the sample, which was followed by the $Cu(Tf_2N)_2$ degradation in the range [100, 250] °C. The final part (T > 250°C) can be associated with the degradation of Cu-IL. The water loss slightly increased at higher RH values, i.e. from 4 to 7.6%, which can be explained by a predominant hydrophobic behavior from $[C_{12}mim][Tf_2N]$ over the hydrophilic copper [49].

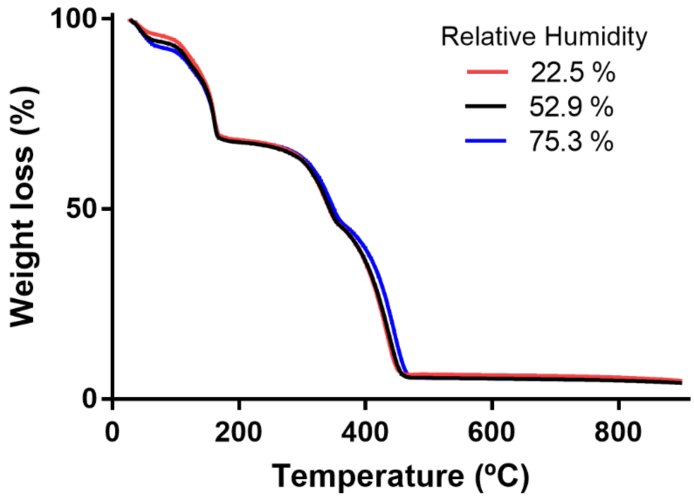

Figure 6. TGA for Cu-IL at three different levels of relative humidity.

Table 2. Cu-IL weight losses at three relative humidity levels.

Relative Humidity	Temperature Range	Weight Loss (%)
22.5 %	25 – 100 °C	4
	100 – 250 °C	27.9
	250 – 900°C	68.1
52.9 %	25 – 100 °C	5.9
	100 – 250 °C	26.7
	250 – 900°C	67.5
75.3 %	25 – 100 °C	7.6
	100 – 250 °C	24.6
	250 – 900°C	67.8

3.2. Electrochemical impedance spectroscopy and temperature measurements

Figure 7 shows the impedance modulus (|Z|) over temperature. The noise below 8 °C is intrinsic to the open circuit condition. After melting, the impedance decreased sharply leading to a closed circuit state. The slow |Z| increase after 12 °C could depend on thermal noise. Figure 8 shows the corresponding output of the RFID reader.

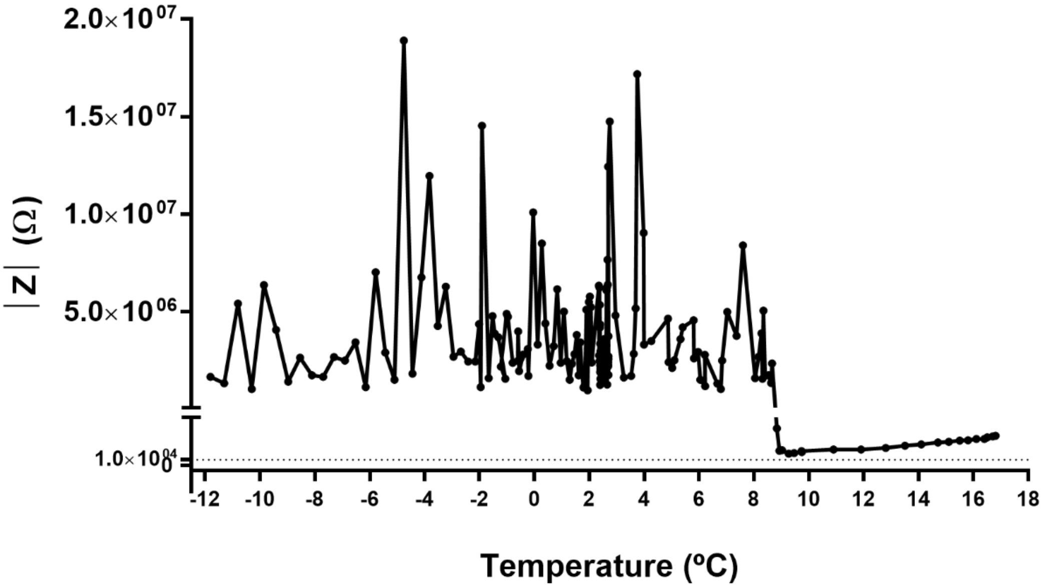

Figure 7. Impedance module of Cu-IL over temperature.

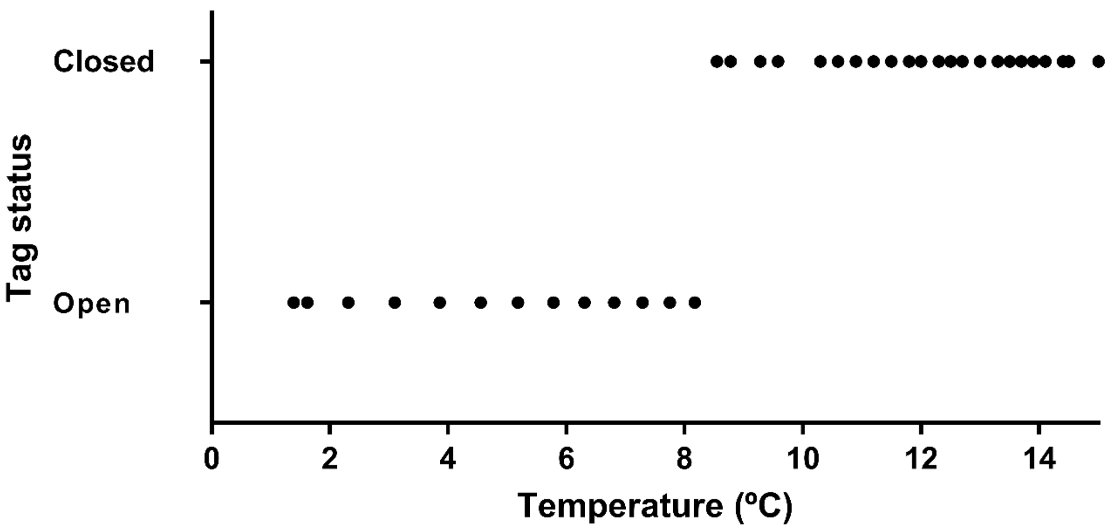

Figure 8. Tag status versus temperature.

4. Conclusion

A modified RFID tag for the identification of failures in the cold chain during transport of temperature-sensitive products has been proposed. The doping of an ionic liquid with copper ions allowed a fine tuning its melting and freezing points, which are remarkably different due to overcooling. We showed how to exploit the irreversible melting of our Cu-IL upon the crossing of the 8 °C threshold to induce a transition in the RFID tag state. The Cu-IL proved stable at different relative humidity levels, which allows the tag to be used in the cold chain system flawlessly. However, enclosure of the tag in a sealed envelope would at the same time avoid interferences from ambient humidity and prevent contamination from copper. A main advantage of using a modified RFID tag relies in the simultaneous acquisition of information from multiple packages from a same reader without any direct or visual contact. The tags can be inexpensive and the threshold temperature is easily tuned by changing the composition of the CU-IL.

Acknowledgements

Regione Toscana and University of Pisa are gratefully acknowledged for supporting this study under the projects eQuality4logistics (POR FESR Toscana 2014-2020) and PRA_2018_26, respectively.

References

[1] Orbis Research, Global Perishable Goods Transportation Market Growth Opportunities and Forecast 2018-2022, 2018.

[2] Grand View Research, Cold Chain Market Size, Share & Trends Analysis Report By Type (Transportation, Monitoring Components, Storage), By Packaging, By Equipment, By Application, By Region, And Segment Forecasts, 2019-2025, 2019.

[3] S. Mercier, S. Villeneuve, M. Mondor, I. Uysal, Time–Temperature Management Along the Food Cold Chain: A Review of Recent Developments, Compr. Rev. Food Sci. Food Saf. 16 (2017) 647–667. doi:10.1111/1541-4337.12269.

[4] S.J. James, C. James, The food cold-chain and climate change, Food Res. Int. 43 (2010) 1944–1956. doi:10.1016/j.foodres.2010.02.001.

[5] World Health Organization (WHO), Annex 5: WHO good distribution practices for pharmaceutical products, WHO Tech. Rep. Ser. 957 (2010) 235–264. https://www.who.int/medicines/areas/quality_safety/quality_assurance/GoodDistributionPracticesTRS957Annex5.pdf.

[6] G.U, Gazzetta Ufficiale Della Repubblica Italiana, Italia, 2000.

[7] EUR-Lex, No Title, (n.d.).

[8] S. Mercier, S. Villeneuve, M. Mondor, I. Uysal, Time–Temperature Management Along the Food Cold Chain: A Review of Recent Developments, Compr. Rev. Food Sci. Food Saf. (2017). doi:10.1111/1541-4337.12269.

[9] FAO, Food wastage footprint. Impacts on natural resources., 2013. doi:ISBN 978-92-5-107752-8.

[10] Pharmaceutical Commerce, The Cold Chain Directory 2015: The 2015 Biopharma Cold Chain Landscape, 2015.

[11] P.S. Taoukis, Application of Time-Temperature Integrators for Monitoring and Management of Perishable Product Quality in the Cold Chain, in: Smart Packag. Technol. Fast Mov. Consum. Goods, 2008: pp. 61–74. doi:10.1002/9780470753699.ch4.

[12] P. Müller, M. Schmid, Intelligent packaging in the food sector: A brief overview, Foods. (2019). doi:10.3390/foods8010016.

[13] V. Kramar, H. Maatta, H. Hinkula, O. Thorsen, G. Cox, Smart-fish system for fresh fish cold chain transportation - Overall approach and selection of sensor materials, in: Conf. Open Innov. Assoc. Fruct, 2018. doi:10.23919/FRUCT.2017.8250183.

[14] A.T.M.M. Rahman, D.H. Kim, H.D. Jang, J.H. Yang, S.J. Lee, Preliminary study on biosensor-type time-temperature integrator for intelligent food packaging, Sensors (Switzerland). (2018). doi:10.3390/s18061949.

[15] Q. Shan, Y. Liu, G. Prossec, D. Brown, Wireless Intelligente Sensors Network for Refrigerated Vehicle, (2004). doi:10.1109/CASSET.2004.1321941.

[16] P.H. Chou, C.T. Lee, Z.Y. Peng, J.P. Li, T.K. Lai, C.M. Chang, C.H. Yang, Y.L. Chen, C.C. Nien, L.H. Chen, L.Y. Lai, J.C. Lu, S.C. Hung, A bluetooth-smart insulating container for cold-chain logistics, Proc. - IEEE 6th Int. Conf. Serv. Comput. Appl. SOCA 2013. (2013) 298–303. doi:10.1109/SOCA.2013.46.

[17] A.A. Zaher, Smart Temperature Sensors: History, Current Practices, and Future Trends, in: Process Anal. Des. Intensif. Microfluid. Chem. Eng. IGI Glob., 2019: p. 28.

[18] S. Wang, J. Tang, F. Younce, Temperature measurement, in: Encycl. Agric. Food, Biol. Eng., 2003: pp. 987 – 993.

[19] P.S. Taoukis, M.C. Giannakourou, T.N. Tsironi, Monitoring and Control of the Cold Chain, in: Handb. Frozen Food Process. Packag. 2nd Ed. Da-Wen Sun (Ed.), CRC Press. Boca Raton, Florida, 2012.

[20] A. Tong, Improving the accuracy of temperature measurements, Sens. Rev. (2001). doi:10.1108/02602280110398044.

[21] B.B. Maskey, J. Sun, K. Shrestha, S. Kim, M. Park, Y. Kim, H. Park, S. Lee, Y. Han, J. Lee, Y. Majima, J. Kim, J. Lee, G. Bahk, G.R. Koirala, G. Cho, A smart food label utilizing roll-

to-roll gravure printed NFC antenna and thermistor to replace existing “use-by” date system, IEEE Sens. J. (2019). doi:10.1109/jsen.2019.2948752.

[22] P.J. McColloster, A. Martin-de-Nicolas, Vaccine refrigeration, Hum. Vaccin. Immunother. (2014). doi:10.4161/hv.27660.

[23] O.C. de Mello Vasconcelos, D. Duarte, J. de Castro Silva, N.F. Oliveros Mesa, B.J. Teruel Mederos, S.T. de Freitas, Modeling ‘Tommy Atkins’ mango cooling time based on fruit physicochemical quality, Sci. Hortic. (Amsterdam). (2019). doi:10.1016/j.scienta.2018.09.068.

[24] A.A. Van Wyk, Assessment of the performance of thermocouple wires vs. thermistor sensors in a cold room. Report to Perishable Products Export Control Board., 2003.

[25] T.G. Claggett, R.W. Worrall, B.G. Lipták, P.M.B. Silva Girão, Thermistors, in: Instrum. Eng. Handbook, Vol. One Process Meas. Anal. CRC Press, 2003.

[26] R. Badia-Melis, U. Mc Carthy, L. Ruiz-Garcia, J. Garcia-Hierro, J.I. Robla Villalba, New trends in cold chain monitoring applications - A review, Food Control. (2018). doi:10.1016/j.foodcont.2017.11.022.

[27] F. Li, Z. Chen, Brief analysis of application of RFID in pharmaceutical cold-chain temperature monitoring system, in: Proc. 2011 Int. Conf. Transp. Mech. Electr. Eng. TMEE 2011, 2011. doi:10.1109/TMEE.2011.6199709.

[28] K. Likar, M. Jevšnik, Cold chain maintaining in food trade, Food Control. (2006). doi:10.1016/j.foodcont.2004.09.009.

[29] E. Abad, F. Palacio, M. Nuin, A.G. de Zárate, A. Juarros, J.M. Gómez, S. Marco, RFID smart tag for traceability and cold chain monitoring of foods: Demonstration in an intercontinental fresh fish logistic chain, J. Food Eng. 93 (2009) 394–399.

doi:10.1016/j.jfoodeng.2009.02.004.

[30] Y. Bo, L. Danyu, Application of RFID in cold chain temperature monitoring system, in: 2009 Second ISECS Int. Colloq. Comput. Commun. Control. Manag. CCCM 2009, 2009. doi:10.1109/CCCM.2009.5270408.

[31] R. Want, An Introduction to RFID Technology, IEEE Pervasive Comput. 5 (2006) 25–33. doi:10.1109/MPRV.2006.2.

[32] P. Nikitin, K.V.S. Rao, S. Lazar, An overview of near field UHF RFID, in: 2007 IEEE Int. Conf. RFID, IEEE RFID 2007, 2007. doi:10.1109/RFID.2007.346165.

[33] K. Opasjumruskit, T. Thanthipwan, O. Sathusen, P. Sirinamarattana, P. Gadmanee, E. Pootarapan, N. Wongkomet, A. Thanachayanont, M. Thamsirianunt, Self-powered wireless temperature sensors exploit RFID technology, IEEE Pervasive Comput. 5 (2006) 54–61. doi:10.1109/MPRV.2006.15.

[34] L. Boquete, R. Cambralla, J.M. Rodrguez-Ascariz, J.M. Miguel-Jimnez, J.J. Cantos-Frontela, J. Dongil, Portable system for temperature monitoring in all phases of wine production, ISA Trans. (2010). doi:10.1016/j.isatra.2010.03.001.

[35] C. Amador, J.P. Emond, M.C. do N. Nunes, Application of RFID technologies in the temperature mapping of the pineapple supply chain, Sens. Instrum. Food Qual. Saf. (2009). doi:10.1007/s11694-009-9072-6.

[36] K. Reiners, A. Hegger, E.F. Hessel, S. Böck, G. Wendl, H.F.A. Van den Weghe, Application of RFID technology using passive HF transponders for the individual identification of weaned piglets at the feed trough, Comput. Electron. Agric. (2009). doi:10.1016/j.compag.2009.05.010.

[37] L. Ruiz-Garcia, L. Lunadei, The role of RFID in agriculture: Applications, limitations and

challenges, Comput. Electron. Agric. (2011). doi:10.1016/j.compag.2011.08.010.

[38] W. Tingman, Z. Jian, Z. Xiaoshuan, Fish product quality evaluation based on temperature monitoring in cold chain, African J. Biotechnol. (2010). doi:10.5897/AJB09.1344.

[39] R. Jedermann, L. Ruiz-Garcia, W. Lang, Spatial temperature profiling by semi-passive RFID loggers for perishable food transportation, Comput. Electron. Agric. 65 (2009) 145–154. doi:10.1016/j.compag.2008.08.006.

[40] R. Bhattacharyya, C. Di Leo, C. Floerkemeier, S. Sarma, L. Anand, RFID tag antenna based temperature sensing using shape memory polymer actuation, in: Proc. IEEE Sensors, 2010. doi:10.1109/ICSENS.2010.5690951.

[41] T. Welton, Room-Temperature Ionic Liquids. Solvents for Synthesis and Catalysis, Chem. Rev. 99 (1999) 2071–2084. doi:10.1021/cr980032t.

[42] T. Schäfer, F. Di Francesco, R. Fuoco, Ionic liquids as selective depositions on quartz crystal microbalances for artificial olfactory systems-a feasibility study, Microchem. J. (2007). doi:10.1016/j.microc.2006.06.001.

[43] F. Di Francesco, C. Ferrari, L. Moni, B. Melai, L. Bernazzani, C. Chiappe, Tuning of the freezing and melting points of [Hmim][NO3] by the addition of water and nitrate salts, RSC Adv. 4 (2014) 40407–40413. doi:10.1039/c4ra06290f.

[44] L. Greenspan, Humidity fixed points of binary saturated aqueous solutions, J. Res. Natl. Bur. Stand. (1934). 81A (1997). doi:10.2307/2406893.

[45] M. Galiński, A. Lewandowski, I. Stepniak, Ionic liquids as electrolytes, Electrochim. Acta. 51 (2006) 5567–5580. doi:10.1016/j.electacta.2006.03.016.

[46] S.M. Murray, T.K. Zimlich, A. Mirjafari, R.A. O'Brien, J.H. Davis, K.N. West, Thermophysical properties of imidazolium-based lipidic ionic liquids, J. Chem. Eng. Data.

58 (2013) 1516–1522. doi:10.1021/je301004f.

[47] C. James, B.A. Onarinde, S.J. James, The Use and Performance of Household Refrigerators : A Review, 16 (2017) 160–179. doi:10.1111/1541-4337.12242.

[48] F. Di Francesco, N. Calisi, M. Creatini, B. Melai, P. Salvo, C. Chiappe, Water sorption by anhydrous ionic liquids, Green Chem. (2011). doi:10.1039/c1gc15080d.

[49] J.G. Huddleston, A.E. Visser, W.M. Reichert, H.D. Willauer, G.A. Broker, R.D. Rogers, Characterization and comparison of hydrophilic and hydrophobic room temperature ionic liquids incorporating the imidazolium cation, Green Chem. 3 (2001) 156–164. doi:10.1039/b103275p.